© 2016. Published by The Company of Biologists Ltd | Development (2016) 143, 2958-2964 doi:10.1242/dev.136739

Live imaging of X chromosome reactivation dynamics in early mouse development can discriminate naïve from primed pluripotent stem cells

Shin Kobayashi[1,‡], Yusuke Hosoi[1], Hirosuke Shiura[1], Kazuo Yamagata[2,*], Saori Takahashi[1], Yoshitaka Fujihara[2], Takashi Kohda[1], Masaru Okabe[2] and Fumitoshi Ishino[1]

ABSTRACT

Pluripotent stem cells can be classified into two distinct states, naïve and primed, which show different degrees of potency. One difficulty in stem cell research is the inability to distinguish these states in live cells. Studies on female mice have shown that reactivation of inactive X chromosomes occurs in the naïve state, while one of the X chromosomes is inactivated in the primed state. Therefore, we aimed to distinguish the two states by monitoring X chromosome reactivation. Thus far, X chromosome reactivation has been analysed using fixed cells; here, we inserted different fluorescent reporter gene cassettes (*mCherry* and *eGFP*) into each X chromosome. Using these knock-in 'Momiji' mice, we detected X chromosome reactivation accurately in live embryos, and confirmed that the pluripotent states of embryos were stable *ex vivo*, as represented by embryonic and epiblast stem cells in terms of X chromosome reactivation. Thus, Momiji mice provide a simple and accurate method for identifying stem cell status based on X chromosome reactivation.

KEY WORDS: X chromosome reactivation, X chromosome inactivation, Live-cell imaging, Pluripotent stem cells, Early mouse development

INTRODUCTION

Silencing of one of the two X chromosomes in female mammals is an epigenetic gene regulatory mechanism known as X chromosome inactivation (XCI). The patterns of XCI change dynamically during early mouse development (Augui et al., 2011; Jeon et al., 2012). From the 4-cell stage on, the paternally derived X chromosome (X_p) is inactivated, referred to as an imprinted XCI. This is carried through to the trophectoderm of blastocysts, and is maintained during trophoblastic differentiation and in the placenta. In the inner cell mass (ICM) of blastocysts, this imprinted XCI is erased, and both X chromosomes become activated, called X chromosome reactivation (XCR). After implantation, either the maternally derived (X_m) or X_p chromosome is silenced in the epiblast, referred to as random XCI. If this mechanism is disturbed, both X chromosomes become transcriptionally active in female embryos, leading to embryonic death after implantation. Therefore, it is believed that XCI occurs in all differentiated cells. However, pluripotent stem cells (PSCs) such as the ICM of blastocysts and embryonic stem cells (ESCs), in addition to primordial germ cells, show reactivation of X chromosomes, resulting in two active ones. Such XCR is also observed during the genomic reprogramming of induced pluripotent stem cells (iPSCs) derived from differentiated cells. Thus, inactivation and reactivation of the X chromosomes are closely linked to the loss and gain of pluripotency, respectively (Pasque and Plath, 2015).

PSCs are useful for studying development and provide important material for therapy because of their ability for self-renewal and differentiation into any cell type. PSCs can be classified into two distinct states: naïve and primed (Nichols and Smith, 2009). These are thought to represent consecutive snap-shots of changes in pluripotency during embryogenesis. In mice, ESCs established from preimplantation embryos represent the naïve state and epiblast stem cells (EpiSCs) established from post-implantation embryos represent the primed state (Nichols and Smith, 2009). These two cell types show different states of pluripotency. When injected into preimplantation embryos, ESCs contribute to form chimeras but EpiSCs do not. However, both types show expression of central pluripotent markers such as the transcription factors *Oct4* and *Sox2* at similar levels, making it difficult to distinguish them. In contrast, these two stem cell types show different epigenetic states of X chromosomes; XCR occurs in ESCs, whereas XCI occurs in EpiSCs. Thus, reactivation of X chromosomes is used as an indicator of naïve-state PSCs (Ohhata and Wutz, 2013; Pasque and Plath, 2015). However, currently there is no means of monitoring XCR in living cells.

Here, we developed a live-cell imaging technique to monitor XCR and examined whether we could accurately detect the dynamics of XCI and XCR changes in early developing embryos. We also tested whether the epigenetic status of the naïve and primed states of pre- and post-implantation embryos were stabilized *ex vivo*, represented by ESCs and EpiSCs in terms of XCR. Finally, we successfully distinguished the two different PSC states using this method.

RESULTS AND DISCUSSION

Live-cell imaging of XCR

To monitor the epigenetic states of both X chromosomes simultaneously in live cells, we inserted CAG promoter-driven reporter gene cassettes encoding two different fluorescent proteins, mCherry and enhanced green fluorescent protein (eGFP), into specific loci (*Pgk1* and *Hprt*) in the X chromosomes (Fig. 1A,B). A recent study has suggested that XCI processes are affected by

[1]Department of Epigenetics, Medical Research Institute, Tokyo Medical & Dental University, 1-5-45 Yushima Bunkyo-ku, Tokyo 113-8510, Japan. [2]Research Institute for Microbial Diseases, Osaka University, Yamadaoka 3-1, Suita, Osaka 565-0871, Japan.
*Present address: KINKI University, Faculty of Biology-Oriented Science and Technology, Department of Genetic Engineering, Nishimitani 930, Kinokawa, Wakayama 649-6493, Japan.

[‡]Author for correspondence (kobayashi.mtt@mri.tmd.ac.jp)

S.K., 0000-0001-6639-3810

Received 25 February 2016; Accepted 8 July 2016

Development (2016) 143, 2958-2964 doi:10.1242/dev.136739

chromosomal topology and the nuclear locality, and are not established uniformly throughout chromosomes (Cerase et al., 2015). Therefore, we expected that different insertion sites of the two reporter genes might provide different monitoring results depending on the time of development and tissues involved. We generated four knock-in (KI) mouse lines with two different insertion sites in combination with two different fluorescent gene markers (Fig. 1B). The *Pgk1* and *Hprt* X-linked loci were chosen to be targets for the reporter genes, because they obey XCI.

As shown in Fig. 2A, a single copy of a CAG promoter driving an *eGFP-NLS* reporter cassette was inserted downstream of the *Pgk1* gene using conventional gene-targeting methods. Recombination was confirmed by polymerase chain reaction (PCR) and Southern blot analyses (Fig. 2B; Fig. S2A,C). The offspring were genotyped by PCR (Fig. 2C). Female mice heterozygous for the $Pgk1^{GFP}$ allele were mated with transgenic male mice expressing FLP recombinase to remove the *Neo* cassette (Fig. 2D). To target the *Hprt* locus, we used a previously reported insertion site (Farhadi et al., 2003); Fig. 2E-G shows the strategy used in generating the $Hprt^{GFP}$ allele. Single-copy insertion was also confirmed at this locus (Fig. S2B,C). The same targeting strategies were used to generate *CAG-mCherry-NLS* reporter cassettes inserted into the *Pgk1* ($Pgk1^{RED}$), and *Hprt* loci ($Hprt^{RED}$), except that we used a Puromycin selection cassette instead of a Neomycin cassette (Fig. S1A-G and Fig. S2A-C).

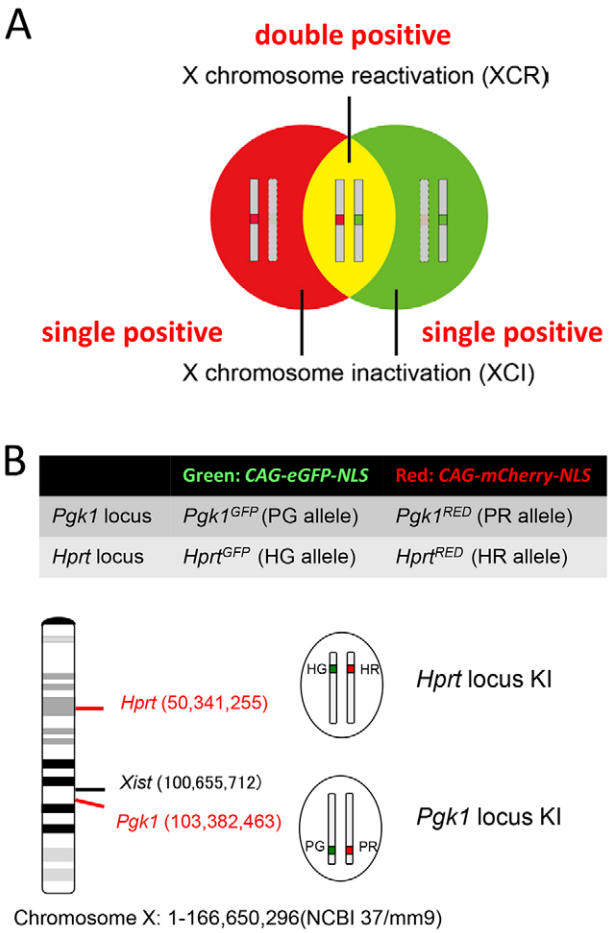

Fig. 1. System of live-cell imaging of X-chromosome reactivation. (A) Two different fluorescent protein reporter genes (*mCherry* and *eGFP*) were inserted into X chromosomes. (B) Two X-linked gene loci (*Hprt* and *Pgk1*) were used for the insertion of reporter gene cassettes encoding the fluorescent protein markers.

Observation of the epigenetic dynamics of both X chromosomes during mouse embryogenesis

To discriminate different types of stem cells, we investigated whether our KI mice were able to display the inactive as well as the active X chromosomes in embryos *in vivo*. We commenced with *Hprt* locus-KI mice to check their status. MCherry-expressing female mice ($Hprt^{RED}$/+) were mated with eGFP-expressing male mice ($Hprt^{GFP}$/Y) and embryonic day (E) 2.5 embryos were recovered from oviducts. These were subjected to time-lapse imaging experiments (Fig. 3A; Movie 1). In early compacted morulae (~16 cells), mCherry signals were barely detectable (E2.5 in Fig. 3A). This indicated that any marker proteins carried over from unfertilized eggs had little effect on subsequent observations. During development from morulae to blastocysts, MCherry signals expressed from the X_m chromosome became apparent but eGFP signals from X_p were barely detected (E2.5 to E4.5 in Fig. 3A). These results were consistent with the reported imprinted XCI pattern. It should be noted that some cells in morulae, as well as trophectoderm cells of blastocysts showed yellowish heterogeneous signals. This suggests that silencing of X_p does not occur in all cells at preimplantation stages, and imprinted XCI was incomplete. The same results were obtained from later embryos recovered from uteri, excluding the possibility of artefacts from the culture conditions (Fig. 3B; morulae and blastocysts). Fig. 3C shows the signal intensities of single cells in a representative embryo corresponding to each developmental stage, suggesting the incompleteness of imprinted XCI in the preimplantation stages. The signal intensity increased as embryos grew to the hatched blastocyst stage and yellowish heterogeneous signals appeared (Fig. 3B,C; morula, mid-stage and hatched blastocysts). We also measured fluorescence in the epiblast of E4.5 embryos (Fig. S3A,B) and confirmed the presence of yellowish cells. However, the reactivation in these cells was not marked compared with the double signals in cells in the epiblast of E5.5 (Fig. 3C; $Hprt^{RED}/Hprt^{GFP}$_E5.5), suggesting that XCR proceeded during the E4.5 to E5.5 stages.

These results were consistent with previous observations in whole embryos using fluorescence *in situ* hybridization to measure X-linked gene expression (Huynh and Lee, 2003; Patrat et al., 2009). In contrast to these conventional methods, our KI mice had the advantage of allowing single-cell resolution. At post-implantation stages on E5.5, cells in the extra-embryonic lineages, including the visceral endoderm (VE) and the extra-embryonic ectoderm (EXE), showed mCherry signals derived from X_m but no eGFP signals from X_p, indicating accurate monitoring of imprinted XCI in these tissues (Fig. 3B, E5.5; Fig. 3C, $Hprt^{RED}/Hprt^{GFP}$_E5.5). On the other hand, epiblast cells at E5.5 showed cells with double signals, implying that XCR was complete by this stage and that the establishment of random XCI was under way (Fig. 3B, E5.5; Fig. 3C, $Hprt^{RED}/Hprt^{GFP}$_E5.5). At E6.5, these cells had disappeared, and either mCherry or eGFP signals were detected in every cell in the epiblasts, indicating that either X_p or X_m had been inactivated randomly. These data show that random XCI was complete by E6.5 (Fig. 3B, E6.5; Fig. 3C, $Hprt^{RED}/Hprt^{GFP}$_E6.5). Consistent with this timing, the *Hprt* gene was reported to be silenced in E6.5 embryos as measured by enzymatic activity (Monk and Harper, 1979). We obtained similar results in the reciprocal crosses between $Hprt^{GFP}$/+ and $Hprt^{RED}$/Y mice

Development (2016) 143, 2958-2964 doi:10.1242/dev.136739

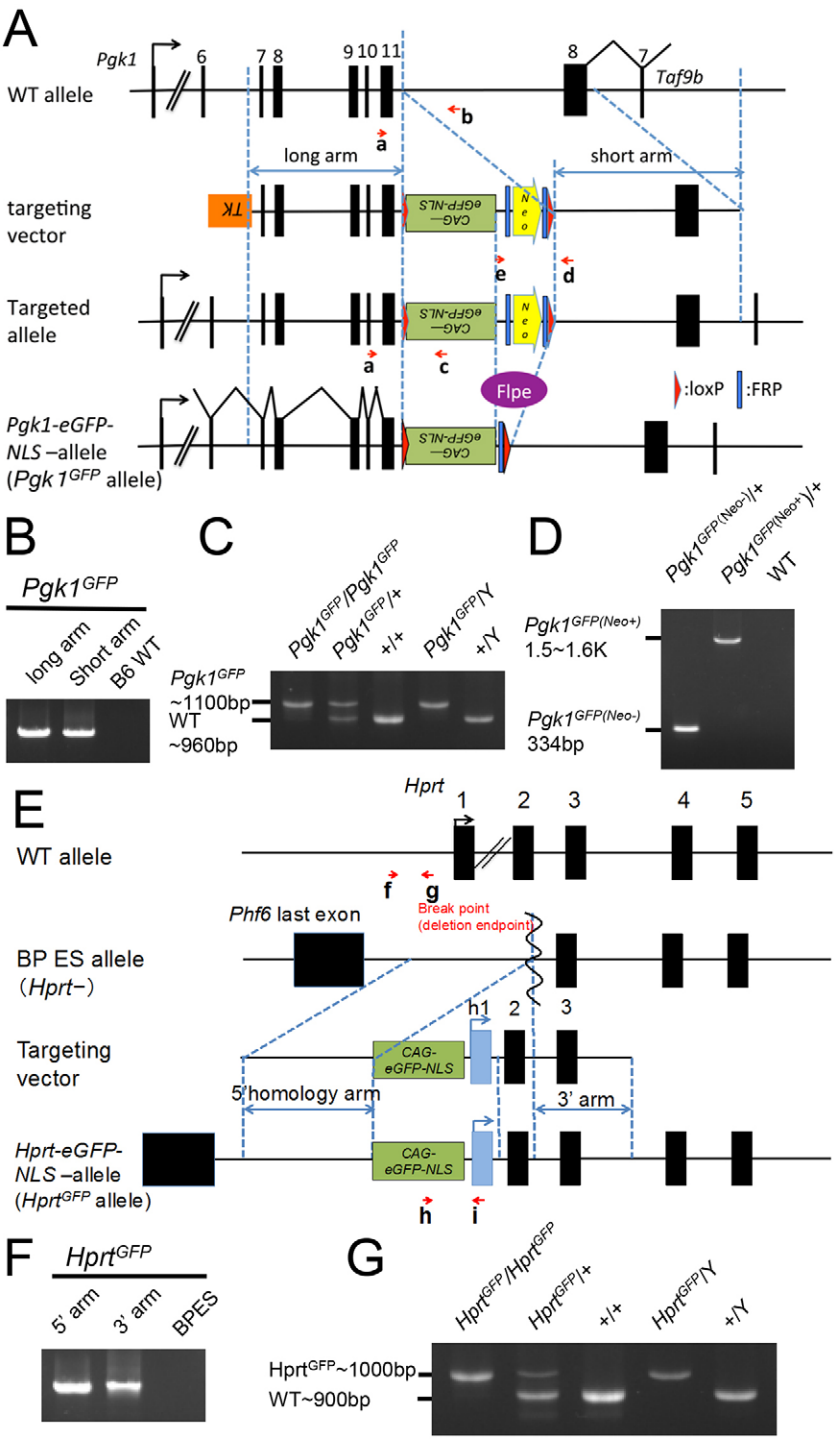

Fig. 2. Generation of Momiji mice. (A) Targeting of *CAG-eGFP-NLS* to the *Pgk1* locus. Complete structures of the targeted alleles are indicated along with the PCR primer positions used for genotyping (red arrows). Flpe, Flip recombinase; TK, thymidine kinase domain. (B) PCR validation of *Pgk1* recombination on the chromosomal target sequences. (C) Genotyping results for homozygous female mice ($Pgk1^{GFP}/Pgk1^{GFP}$), hemizygous female mice ($Pgk1^{GFP}/+$), wild-type (WT) female mice (+/+), hemizygous male mice ($Pgk1^{GFP}/Y$) and WT male mice (+/Y). (D) Confirmation of the excision of the flippase recognition target (FRT)-flanked *Neo* cassette. (E) Targeting of *CAG-eGFP-NLS* to the *Hprt* locus showing the complete structures of the targeted alleles with the PCR primer positions used (arrows). (F) PCR validation of *Hprt* recombination on the chromosomal target sequences. (G) Genotyping results for homozygous female mice ($Hprt^{GFP}/Hprt^{GFP}$), hemizygous female mice ($Hprt^{GFP}/+$), WT female mice (+/+), hemizygous male mice ($Hprt^{GFP}/Y$) and WT male mice (+/Y).

(Fig. S3C,D), and also in crosses using the *Pgk1* locus-KI mice (Fig. S3E-J). However, in the *Pgk1* KI mice, random XCI was slightly delayed at E6.5 (Fig. 3C, $Pgk1^{RED}/Pgk1^{GFP}$_E6.5; Fig. S3J). This delay was also observed in assays using enzymatic activity (McMahon and Monk, 1983). Thus, our live imaging methods successfully detected the positional effects of X-linked genes during XCI *in vivo*. At preimplantation stages, we could not rule out the possibility that incomplete imprinted XCI might be ascribed to the nature of the transgene driven by heterologous CAG, which is known to be a strong promoter. However, the results were consistent with reported XCI patterns (Huynh and Lee, 2003; McMahon and Monk, 1983; Monk and Harper, 1979; Patrat et al., 2009). These KI mice helped us to investigate the dynamics of XCI as well as XCR at a single-cell level. We named this mouse strain 'Momiji' after the leaves of the Japanese maple, which are tinged with red, green and yellow in autumn.

Distinguishing naïve from primed PSCs using Momiji mice

Next, we tried to distinguish naïve from primed stem cells using Momiji $Hprt^{RED}/Hprt^{GFP}$ female mice. First, we established ESCs from blastocysts using a standard protocol (Ying et al., 2008).

Development (2016) 143, 2958-2964 doi:10.1242/dev.136739

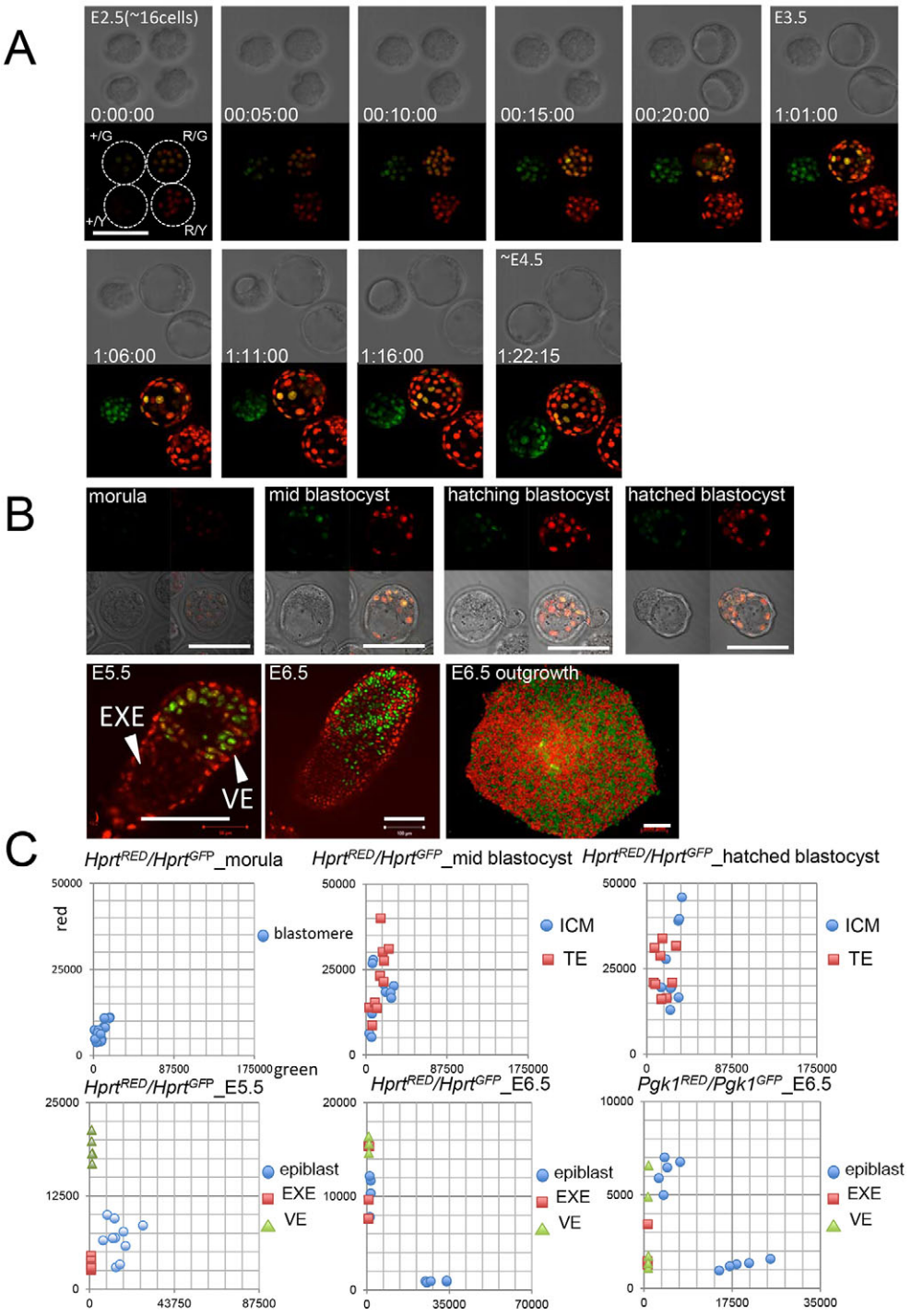

Fig. 3. Dynamic changes in X chromosome inactivation status during early mouse development. Four embryos collected at E2.5 were followed to E4.5. Selected bright-field (top) and fluorescence (bottom) images are shown for every 5 h. Genotypes of the embryos are indicated in the first fluorescence image. G, $Hprt^{GFP}$; R, $Hprt^{RED}$. (B) Morula, mid blastocyst, hatching blastocyst, hatched blastocyst, E5.5, E6.5 recovered from oviducts and/or uterus and cultured at E6.5 for outgrowth. EXE, extra-embryonic ectoderm; VE, visceral endoderm. (C) Quantitative analysis of XCR and XCI in embryos at single-cell resolution. Each spot corresponds to a single cell in an embryo. Genotypes of the samples and developmental stages are indicated on the top of the graph. By convention, the maternal allele precedes the paternal allele for genotypes. The graphs shows representative results. At least two embryos were analysed for each stage. Scale bars: 100 µm.

Established ESCs showed double fluorescence, indicating that both of the X chromosomes were active, and that these cells represented XCR in blastocysts (Fig. 4A). Next, we established EpiSCs from E6.5 embryos using N2B27-based medium supplemented with activin A, basic fibroblast growth factor and the Wnt signalling inhibitor, XAV939 (Sumi et al., 2013) and confirmed that the established cells were in a primed state by examining several markers; alkaline phosphatase staining confirmed that signals in EpiSCs were weaker than in ESCs (Fig. S4A). Immunostaining revealed that EpiSCs exhibited a differentiated epigenetic feature, namely the staining of one X chromosome with the silencing mark H3K27 trimethylation (Fig. S4B, red) and *Xist* (Fig. 4A). Microarray analysis confirmed that these EpiSCs expressed the central pluripotency factors *Oct4*, *Sox2* and *Nanog* at similar levels to ESCs, but EpiSCs had lower levels of many pluripotency-associated transcription factors than did ES cells (e.g. *Rex1*, *Tbx3* and *Fbxo15*), and they showed upregulation of early lineage specification markers such as *Fibroblast growth factor 5* (*Fgf5*) (Fig. S4C). All these data indicate that our EpiSCs were in a primed state of pluripotency.

As expected, the established EpiSCs showed either mCherry or eGFP fluorescence, indicating that random XCI had occurred (Fig. 3B, E6.5 embryonic outgrowth; Fig. 4A, EpiSC). Clearly, our Momiji mice could display the epigenetic status of naïve and

Development (2016) 143, 2958-2964 doi:10.1242/dev.136739

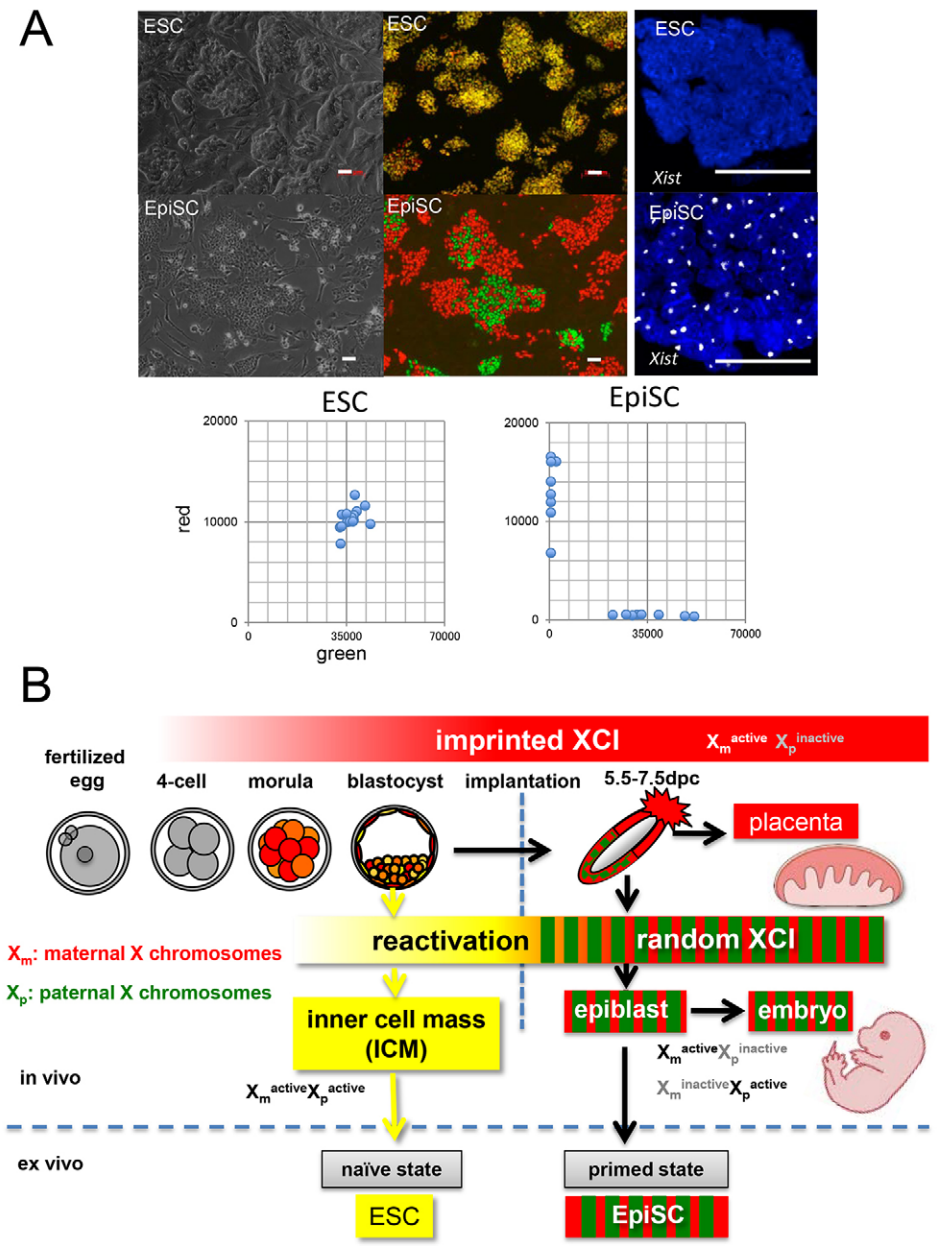

Fig. 4. The epigenetic state of XCR and XCI in mouse development is faithfully reflected in stem cell lines. (A) Two distinct stem cell lines, ESCs and EpiSCs are established from Momiji embryos ($Hprt^{RED}/Hprt^{GFP}$). The panels on the right show confirmation of *Xist* expression using RNA fluorescence *in situ* hybridization (FISH). *Xist*, white; DAPI, blue. (B) Momiji mice can be used to monitor the dynamics of X chromosome activity in mouse development and in stem cell lines established from corresponding embryonic stages of development.

primed PSCs from their XCR state, corresponding to pre- and post-implantation stage embryos.

Advantages and future research perspectives for Momiji mice

There have been several trials monitoring XCI in live cells. XCI has also been studied using transgenic mice carrying X chromosomes tagged with randomly inserted *eGFP* reporters (Hadjantonakis et al., 2001; Kobayashi et al., 2010, 2006, 2013; Nakanishi et al., 2002; Okabe et al., 1997). This mouse strain has an advantage in that one can observe XCI noninvasively and it can be used to monitor the activity of only one of the X chromosomes. However, it cannot be used to detect the activities of both X chromosomes, simultaneously. Therefore, it does not allow researchers to observe XCR in ICMs at the blastocyst stage as well as in naïve-state pluripotent ESCs, or random XCI affecting either the X_p or X_m in post-implantation embryos. Mice expressing GFP and tdTomato have been used to monitor random XCI (Wu et al., 2014). However, there are no reports that monitor XCR in live cells. Here, we succeeded in tracking XCR in living embryos using our Momiji mice and demonstrated that this strain is useful for distinguishing naïve from primed pluripotent stem cells.

Momiji mice offer advantages in stem cell research, including studies on genomic reprogramming, as well as in developmental biology. In terms of the reprogramming of iPSCs, a combination of chemical and genetic manipulations can enable EpiSCs to be converted to naïve iPSCs (Guo et al., 2009; Hanna et al., 2009). XCR occurred during these reprogramming events, but the mechanisms involved have not been clarified. Our data suggest that the Momiji mouse strain will provide a powerful tool for tracing the reprogramming involved in establishing iPSCs (EpiSCs→iPSCs) and will help to clarify how XCR participates in this process. Clarification of the reprogramming processes, from a primed to a naïve state, will help in the effective establishment of naïve human iPSCs from primed ESCs (Dodsworth et al., 2015; Pera, 2014).

Development (2016) 143, 2958-2964 doi:10.1242/dev.136739

MATERIALS AND METHODS

Animals

All experiments were performed according to the guidelines of the Committee on the Use of Live Animals in Teaching and Research of Tokyo Medical and Dental University.

Hprt locus KI mice

The NLS derived from the human MBD1 protein (Ueda et al., 2014) was fused to the N-termini of eGFP and mCherry proteins to generate reporter fluorescent protein cassettes (*CAG-mCherry-NLS*, and *CAG-eGFP-NLS*). These were transferred into a vector targeting *Hprt* (Celtikci et al., 2008). The targeting constructs were then transfected into BPES11 cells and hypoxanthine/aminopterin/thymidine-resistant clones were recovered. To generate chimeras, selected ES cells were injected into 8-cell mouse embryos. KI mice were maintained by crossing to C57BL/6N (Clea, Japan).

Pgk1 locus KI mice

The targeting vector was constructed to insert the reporter cassette into a 380 bp sequence downstream of the *Pgk1* gene. The targeting vectors (pNT1.1) (Tokuhiro et al., 2012) were linearized and electroporated into C57BL/6N ES cells (EGR-G101) (Fujihara et al., 2013). Selected ES cells were subsequently injected into 8-cell stage Slc:ICR strain embryos to generate chimeric mice. KI mice were maintained by crossing to C57BL/6N (Clea, Japan). All PCR primers used in this study are listed in Table S1. These KI mice are available from RIKEN BioResource Center.

Embryo collection

Eight- to 16-week-old $Hprt^{RED}$/+ female mice were mated with $Hprt^{GFP}$ male mice ($Hprt^{GFP}$/Y) for embryo collection. Embryos were collected from the oviducts or uterus and were staged on the basis of their morphology (Downs and Davies, 1993). $Pgk1^{RED}$/+ female mice and $Pgk1^{GFP}$/Y male mice were used for mating. In experiments using reciprocal crosses, eGFP-expressing female mice were mated with mCherry-expressing male mice.

Time-lapse motion imaging of preimplantation embryos

Live-cell imaging of preimplantation embryos was performed as described previously (Yamagata and Ueda, 2013).

Derivation and characterization of EpiSCs and ESCs

EpiSC lines were established from E6.5 epiblasts and ESCs from E3.5 blastocysts using standard methods as detailed in the supplementary Materials and Methods.

Fluorescence *in situ* hybridization (FISH)

Xist RNA FISH was performed as described previously (Soma et al., 2014).

Signal quantification

Observation and quantification of fluorescence signals from embryos and stem cells was performed using a Zeiss LSM 710 confocal microscope. Images were processed using Zeiss ZEN software as described in the supplementary Materials and Methods.

Immunocytochemistry

Alkaline phosphatase activity was detected using a Blue alkaline phosphatase substrate kit (Vector Laboratories). For immunofluorescence staining, cultured cells were fixed in 4% paraformaldehyde in phosphate-buffered saline at 4°C for 15 min and blocked in 1% BSA at room temperature for 1 h. The cells were stained with goat anti-mouse Oct3/4 antibody (Santa Cruz, sc-8628, 1:300) and rabbit anti-mouse H3K27me3 antibody (Upstate, 07-499, 1:1000) at 4°C overnight. Alexa Fluor 488-conjugated donkey anti-goat IgG and Alexa Fluor 568-conjugated goat anti-rabbit IgG (Molecular Probes, A11055, A10042, respectively; both 1:1000) were used as the secondary antibodies. Subsequently, the cells were counterstained with DAPI.

Microarray analysis

Total RNA was isolated from ~2×10^5 cells using TRIzol (Invitrogen). Analysis was performed using Mouse GE microarray kits (4×44K v.2, Agilent Technologies). Gene expression levels of EpiSCs were normalized against the total expression levels of all the autosomal genes in the control cell lines. NCBI (http://www.ncbi.nlm.nih.gov) data for mESCs (GSM1132971 and GSM1132972) and EpiSCs (GSM1962980 and GSM1962981) were used in this study.

Acknowledgements

We thank Dr A. Peterson for providing the *Hprt* targeting vector and BPESCs; Drs S. Ohtsuka and H. Niwa (RIKEN, CDB) for advice on the establishment of EpiSCs; NPO Biotechnology Research and Development for technical assistance in generating the KI mice; and Drs K. Abe and M. Sugimoto at RIKEN BioResource Center for providing the p*Xist* 1986-9498 plasmid, and the anti-Oct4 antibody.

Competing interests

The authors declare no competing or financial interests.

Author contributions

S.K. conceived, designed and performed the experiments, assisted by Y.H., H.S., K.Y., S.T., Y.F., T.K., M.O. and I.F.; S.K., Y.F. and M.O. generated the KI mice; Y.K. carried out time-lapse imaging; S.K. and S.T. characterized the established EpiSCs; S.K., Y.H. and H.S. analysed the early embryos and stem cells; S.K., M.O., T.K. and F.I. wrote the manuscript and all authors discussed the results and commented on the manuscript.

Funding

This work was supported by the Japan Science and Technology Agency, Precursory Research for Embryonic Science and Technology (PRESTO) and by a Grant-in-Aid for Scientific Research from the Ministry of Education, Culture, Sports, Science, and Technology [23500492, 15H01468] to S.K. The funding bodies had no roles in the study design, data collection and analysis, decision to publish or preparation of the manuscript.

Supplementary information

Supplementary information available online at
http://dev.biologists.org/lookup/doi/10.1242/dev.136739.supplemental

References

Augui, S., Nora, E. P. and Heard, E. (2011). Regulation of X-chromosome inactivation by the X-inactivation centre. *Nat. Rev. Genet.* **12**, 429-442.

Celtikci, B., Leclerc, D., Lawrance, A. K., Deng, L., Friedman, H. C., Krupenko, N. I., Krupenko, S. A., Melnyk, S., James, S. J., Peterson, A. C. et al. (2008). Altered expression of methylenetetrahydrofolate reductase modifies response to methotrexate in mice. *Pharmacogenet. Genomics* **18**, 577-589.

Cerase, A., Pintacuda, G., Tattermusch, A. and Avner, P. (2015). Xist localization and function: new insights from multiple levels. *Genome Biol.* **16**, 166.

Dodsworth, B. T., Flynn, R. and Cowley, S. A. (2015). The current state of naïve human pluripotency. *Stem Cells* **33**, 3181-3186.

Downs, K. M. and Davies, T. (1993). Staging of gastrulating mouse embryos by morphological landmarks in the dissecting microscope. *Development* **118**, 1255-1266.

Farhadi, H. F., Lepage, P., Forghani, R., Friedman, H. C., Orfali, W., Jasmin, L., Miller, W., Hudson, T. J. and Peterson, A. C. (2003). A combinatorial network of evolutionarily conserved myelin basic protein regulatory sequences confers distinct glial-specific phenotypes. *J. Neurosci.* **23**, 10214-10223.

Fujihara, Y., Kaseda, K., Inoue, N., Ikawa, M. and Okabe, M. (2013). Production of mouse pups from germline transmission-failed knockout chimeras. *Transgenic Res.* **22**, 195-200.

Guo, G., Yang, J., Nichols, J., Hall, J. S., Eyres, I., Mansfield, W. and Smith, A. (2009). Klf4 reverts developmentally programmed restriction of ground state pluripotency. *Development* **136**, 1063-1069.

Hadjantonakis, A.-K., Cox, L. L., Tam, P. P. L. and Nagy, A. (2001). An X-linked GFP transgene reveals unexpected paternal X-chromosome activity in trophoblastic giant cells of the mouse placenta. *Genesis* **29**, 133-140.

Hanna, J., Markoulaki, S., Mitalipova, M., Cheng, A. W., Cassady, J. P., Staerk, J., Carey, B. W., Lengner, C. J., Foreman, R., Love, J. et al. (2009). Metastable pluripotent states in NOD-mouse-derived ESCs. *Cell Stem Cell* **4**, 513-524.

Huynh, K. D. and Lee, J. T. (2003). Inheritance of a pre-inactivated paternal X chromosome in early mouse embryos. *Nature* **426**, 857-862.

Jeon, Y., Sarma, K. and Lee, J. T. (2012). New and Xisting regulatory mechanisms of X chromosome inactivation. *Curr. Opin. Genet. Dev.* **22**, 62-71.

Kobayashi, S., Isotani, A., Mise, N., Yamamoto, M., Fujihara, Y., Kaseda, K., Nakanishi, T., Ikawa, M., Hamada, H., Abe, K. et al. (2006). Comparison of gene expression in male and female mouse blastocysts revealed imprinting of the X-linked gene, *Rhox5*/*Pem*, at preimplantation stages. *Curr. Biol.* **16**, 166-172.

Kobayashi, S., Fujihara, Y., Mise, N., Kaseda, K., Abe, K., Ishino, F. and Okabe, M. (2010). The X-linked imprinted gene family *Fthl17* shows predominantly female expression following the two-cell stage in mouse embryos. *Nucleic Acids Res.* **38**, 3672-3681.

Kobayashi, S., Totoki, Y., Soma, M., Matsumoto, K., Fujihara, Y., Toyoda, A., Sakaki, Y., Okabe, M. and Ishino, F. (2013). Identification of an imprinted gene cluster in the X-inactivation center. *PLoS ONE* **8**, e71222.
McMahon, A. and Monk, M. (1983). X-chromosome activity in female mouse embryos heterozygous for Pgk-1 and Searle's translocation, T(X; 16) 16H. *Genet. Res.* **41**, 69-83.
Monk, M. and Harper, M. I. (1979). Sequential X chromosome inactivation coupled with cellular differentiation in early mouse embryos. *Nature* **281**, 311-313.
Nakanishi, T., Kuroiwa, A., Yamada, S., Isotani, A., Yamashita, A., Tairaka, A., Hayashi, T., Takagi, T., Ikawa, M., Matsuda, Y. et al. (2002). FISH analysis of 142 *EGFP* transgene integration sites into the mouse genome. *Genomics* **80**, 564-574.
Nichols, J. and Smith, A. (2009). Naive and primed pluripotent states. *Cell Stem Cell* **4**, 487-492.
Ohhata, T. and Wutz, A. (2013). Reactivation of the inactive X chromosome in development and reprogramming. *Cell. Mol. Life Sci.* **70**, 2443-2461.
Okabe, M., Ikawa, M., Kominami, K., Nakanishi, T. and Nishimune, Y. (1997). 'Green mice' as a source of ubiquitous green cells. *FEBS Lett.* **407**, 313-319.
Pasque, V. and Plath, K. (2015). X chromosome reactivation in reprogramming and in development. *Curr. Opin. Cell Biol.* **37**, 75-83.
Patrat, C., Okamoto, I., Diabangouaya, P., Vialon, V., Le Baccon, P., Chow, J. and Heard, E. (2009). Dynamic changes in paternal X-chromosome activity during imprinted X-chromosome inactivation in mice. *Proc. Natl. Acad. Sci. USA* **106**, 5198-5203.
Pera, M. F. (2014). In search of naivety. *Cell Stem Cell* **15**, 543-545.
Soma, M., Fujihara, Y., Okabe, M., Ishino, F. and Kobayashi, S. (2014). Ftx is dispensable for imprinted X-chromosome inactivation in preimplantation mouse embryos. *Sci. Rep.* **4**, 5181.
Sumi, T., Oki, S., Kitajima, K. and Meno, C. (2013). Epiblast ground state is controlled by canonical Wnt/beta-catenin signaling in the postimplantation mouse embryo and epiblast stem cells. *PLoS ONE* **8**, e63378.
Tokuhiro, K., Ikawa, M., Benham, A. M. and Okabe, M. (2012). Protein disulfide isomerase homolog PDILT is required for quality control of sperm membrane protein ADAM3 and male fertility. *Proc. Natl. Acad. Sci. USA* **109**, 3850-3855.
Ueda, J., Maehara, K., Mashiko, D., Ichinose, T., Yao, T., Hori, M., Sato, Y., Kimura, H., Ohkawa, Y. and Yamagata, K. (2014). Heterochromatin dynamics during the differentiation process revealed by the DNA methylation reporter mouse, MethylRO. *Stem Cell Rep.* **2**, 910-924.
Wu, H., Luo, J., Yu, H., Rattner, A., Mo, A., Wang, Y., Smallwood, P. M., Erlanger, B., Wheelan, S. J. and Nathans, J. (2014). Cellular resolution maps of X chromosome inactivation: implications for neural development, function, and disease. *Neuron* **81**, 103-119.
Yamagata, K. and Ueda, J. (2013). Long-term live-cell imaging of mammalian preimplantation development and derivation process of pluripotent stem cells from the embryos. *Dev. Growth Differ.* **55**, 378-389.
Ying, Q.-L., Wray, J., Nichols, J., Batlle-Morera, L., Doble, B., Woodgett, J., Cohen, P. and Smith, A. (2008). The ground state of embryonic stem cell self-renewal. *Nature* **453**, 519-523.